SPE 115361

Improved Prediction of Oil Recovery from Waterflooded Fractured Reservoirs Using Homogenization

Hamidreza Salimi, SPE, and Johannes Bruining, SPE, Delft University of Technology

This paper was prepared for presentation at the 2008 SPE Annual Technical Conference and Exhibition held in Denver, Colorado, USA, 21–24 September 2008.

Abstract

Most simulations of waterflooding in fractured media are based on the Warren and Root (WR) approach, which uses an empirical transfer function between the fracture and matrix block. Arbogast used homogenization to formulate an improved flow model in fractured media, leading to an integro-differential equation; also called the boundary condition (BC) approach. A well-posed numerical 3D model for the BC approach has been formulated. This paper derives this numerical model to solve full 3D integro-differential equations in a field reservoir simulation. The results of this model are compared with ECLIPSE results. For the interpretation, it is useful to define three dimensionless parameters, which characterize the oil production in fractured media. The most important of these parameters is a Peclet number defined as the ratio between the time required to imbibe water into the matrix block and the travel-time of water in the fracture system. The results of the WR approach and the BC approach are in good agreement when the travel-time is longer than the imbibition time. However, if the travel time is shorter than the imbibition time or of the same order of magnitude, the approaches give different results. The BC approach allows the use of transfer functions based on fundamental principles, e.g., the use of a rate-dependent capillary-pressure function. When implemented, it can be used to improve recovery predictions for waterflooded fractured reservoirs.

Introduction

Naturally fractured petroleum reservoirs represent over 20% of the world's oil and gas reserves (Saidi 1983), but are among the most complicated class of reservoirs to produce efficiently. Naturally fractured reservoirs (NFR's) comprise an interconnected fracture system that provides the main flow paths and the reservoir rock or matrix that acts as the main source of hydrocarbons.

From the geological point of view, it is possible to distinguish between various types of fractured reservoirs (Nelson 1985; Stearns 1969; Stearns 1972). The most important aspect is whether the fracture network provides a continuous flow path (Saidi 1983) or whether it has regions with different fracture geometries or systems consisting of a hierarchy of fracture systems at different scales (multi-scale fractures) (Yu-Shu Wu 2004; Gasem et al. 2008). When the fracture network is not continuous, the reservoir can be split up in fractured and non-fractured domains. Also in the fractured domains, the reservoir is heterogeneous, with different fracture densities, fracture apertures, anisotropies etc. In some approximate sense, the fractured reservoirs show some repetition of fractured sub-domains. This aspect will be used for obtaining averaged properties of the sub-domains. The same idea can also be used as a first guess to obtain the global flow field. Alternatively, it is possible to use the global flow field to obtain boundary conditions at the local scale and repeat this procedure until convergence has been obtained.

Flow modeling in fractured reservoirs was greatly advanced by Barenblatt et al. (1960), who introduced the concept of "dual porosity," In addition, he introduced the transfer function and shape factor. From the geometrical point of view, Barenblatt assumed that the fracture system is regular "to some extent," Warren and Root (1963) used the dual-porosity model and applied it to a well-test analysis. They also introduced the sugar cube model, which has been the basis of many of the fractured reservoir simulators since that time. The dual-porosity model of Warren and Root for examining pressure drawdown and buildup phenomena in NFR's was extended by Kazemi et al. (1969, 1992) to interpret interference test results. These ideas were extended with the introduction of the so-called dual-permeability model, where the matrix blocks can also contribute to the global flow, depending on the permeability ratio of fractures and matrix blocks.

The transfer function is semi-empirical. It relates the fluid flow at the interface between matrix and fracture to the driving force, e.g., average phase pressure difference between fracture and matrix. More recently, the ideas were extended with the derivation of transfer functions based on fundamental transport modeling. Dutra and Aziz (1992) presented a model that takes

into account the transient nature of the imbibition process and the effect of variation in fracture saturation. Sarma and Aziz (2006) proposed a general numerical technique to calculate the shape factor for any arbitrary shape of the matrix block, i.e., non-orthogonal fractures.

One drawback is that the transfer-function approach ignores the history-dependent nature of the transfer process. This would be only justified if the time-dependence of the boundary condition around the matrix block is weak.

A new approach was introduced by Douglas and Arbogast (1989, 1990, 1991), where they applied a new upscaling technique (homogenization) to derive the model equations for flow in fractured reservoirs, which does not suffer from the above-mentioned drawback. Full derivations can be found in Arbogast (1993a, 1993b, 1997) and Arbogast and Lehr (2006). These papers were written for a mathematically oriented audience.

The following brief description of homogenization for fractured media emphasizes the physics. A microscopic transport model in a fractured medium consists of (1) the flow equations in the fracture, (2) the flow equations in the matrix and (3) the boundary conditions between matrix and fracture, i.e., continuity of capillary pressure (unless one of the phases is at residual saturation) and continuity of flux. Application of homogenization leads to a transport equation in the fracture system with a source term that describes the amount of oil that is transferred from the matrix blocks to the fracture. Homogenization suggests that for the calculation of the source term we need to solve the two-phase flow equations in the matrix block subject to a boundary potential that is given by the potential of the fracture system on the macro-scale. Therefore, this potential for a single matrix block can depend on time and the space coordinates. One of the assumptions used in homogenization is that the order of magnitude of each term in the transport equations can be related to a single scaling parameter (ε). This scaling parameter describes the ratio of the local scale and the global scale. This means that the order of magnitude of all characteristic dimensionless numbers must be expressed in terms of this scaling ratio. The second assumption is that the domain can be subdivided in parts (unit cells) in which the flow equations can be solved using periodic boundary conditions. This implies that a condition for the application of homogenization is that the separation of scales is possible. After averaging the equations over the unit cell, we find the upscaled equations. Different upscaled model equations are obtained when different orders of magnitudes for the dimensionless parameters are used. This allows the definition of sub-domains in the parameter space that give qualitatively different behavior. It is the purpose of this paper to quantify these regimes of different behavior based on a characteristic dimensionless number. For problems of engineering interest, these orders of magnitude can be easily assigned. To illustrate the advantages and disadvantages of the boundary condition approach (homogenization), we compare it with Warren Root approach using ECLIPSE. The main advantage of homogenization is that it allows deriving the exchange rate between matrix and fracture based on first principles.

We ignored the time-dependent boundary conditions for the matrix block in a previous paper (Namdar Zanganeh et al. 2007). This paper shows how to incorporate the time-dependent boundary conditions for the matrix block. It also stresses other aspects, i.e., the definition and importance of characteristic numbers. Moreover, it uses a fully implicit approach to solve the model equations, which now include gravity.

The paper is organized as follows: Section 1 describes the general framework of homogenization based on a physical model for a fractured reservoir. Section 2 introduces the dimensionless numbers. Here, we also define a Peclet number as a ratio between the time of capillary diffusion of oil from the matrix to the fracture and the residence time of water in the reservoir. The results, presented in section 3, are interpreted in terms of the dimensionless groups. We end with some conclusions. Appendix A shows the derivation of the effective fracture permeability tensor. Appendix B gives the full 3-D numerical model.

1. Methodology of homogenization

1.1. Physical model

Consider a fracture network with matrix blocks in between. The matrix blocks are completely surrounded by fractures except for some isolated crushed zones with zero permeability holding the matrix blocks together. The local fracture porosity and intrinsic permeability evaluated inside the fracture are denoted by φ_f^* and k_f^*, respectively. We define the intrinsic fracture permeability k_f^* based on the fracture aperture. As the main purpose of this paper is to illustrate only the essential concepts, we assume here that the symmetry of the fracture pattern is such that the fracture permeability can be considered isotropic but this assumption can be easily relaxed (see appendix A). The global fracture porosity and effective permeability evaluated with respect to the bulk volume are denoted by φ_f and k_f, respectively. The matrix porosity and matrix permeability are denoted by φ_m and k_m. Note that small differences between intrinsic and global values of the matrix porosity and permeability are ignored, and only the global values are used here. We consider only two-phase (oil and water) incompressible flow where the water viscosity μ_w and oil viscosity μ_o, are assumed constant. We use the two-phase (α = o, w) extension of Darcy's law for constant fluid densities:

$$\mathbf{u}_{\alpha f}^* = -\frac{k_f^* k_{r\alpha,f}}{\mu_\alpha}\nabla\left(P_{\alpha f} + \rho_\alpha g z\right) := -\lambda_{\alpha f}^* \nabla\Phi_{\alpha f}, \qquad \text{and} \qquad \mathbf{u}_{\alpha m} = -\frac{k_m k_{r\alpha,m}}{\mu_\alpha}\nabla\Phi_{\alpha m} := -\lambda_{\alpha m}\nabla\Phi_{\alpha m}. \tag{1}$$

In these equations the superscript (*) denotes the intrinsic fracture properties. Here z is the vertically upward direction. Note that the fracture permeability and matrix permeability are considered isotropic. Relative permeabilities are denoted by $k_{rw\zeta}$ and

$k_{ro\zeta}$, where ζ indicates the fracture and matrix systems. In the same way, $P_{c\zeta}$ denotes the capillary pressure. There is capillary pressure continuity at the boundary of fractures and matrix blocks unless one of the phases either in the matrix or in fracture is immobile (Duijn et al. 1995). Indeed when one of the phases is immobile, the pressure of that phase depends on local conditions and cannot be determined globally. Hence, the capillary pressure, which is the difference between the phase pressure of the nonwetting phase and wetting phase, is not continuous. However, as residual saturations do not flow, this has no relevance for the modeling. Continuity of force, and hence continuity of phase pressures, implies continuity of capillary pressure when both phases are mobile.

The disparity of permeability between the fracture and matrix has a consequence that only a small deviation from connate water saturation in the fracture leads to a water saturation close to 1-S_{or} in the part of the matrix adjacent to the fracture.

1.2. Homogenization procedure

The homogenization procedure is divided into four major steps, based on specific assumptions that are stated in each step. We deviate somewhat from the conventional description of homogenization by de-emphasizing the central role of periodicity. In our view, this is only a minor issue.

The first step in the homogenization is subdividing the fractured reservoir into two scales (see **Fig. 1**): local (small units) scale of size (l) and the global scale of size (L) that is much larger than the local scale. Our choice for the small units (SU) scale is a single matrix block surrounded by fractures, but it is also possible to choose a more complex structure with several matrix blocks for the small-units scale. We define L as the dimension of the reservoir because the fractured reservoir of our choice is homogeneous in some averaged sense. However, if the fractured reservoir is locally heterogeneous, it is possible to define L as the dimension of the grid block length. A very large difference between the size of the global scale (reservoir) and the local scale (SU) in addition to the low permeability of matrix blocks, suggests that the oil flux from the matrix blocks to fractures will only lead to local scale variations of the fracture potential. We define a scaling ratio $\varepsilon = l / L$ between the local scale and the global scale.

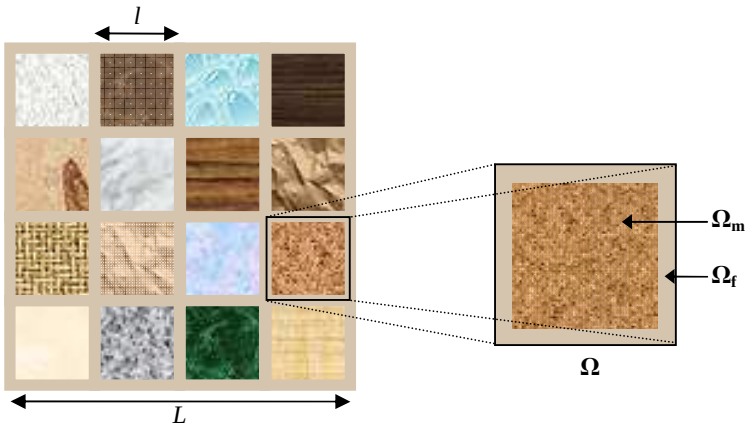

Fig. 1- The global scale, (left). The local scale (small unit), (right)

Therefore, we consider the medium as an aggregate of SU's, in which each unit cell consists of a matrix block surrounded by fractures. Fig.1 also illustrates our assumption that the fractured reservoir consists of a continuous network of fractures with isolated matrix blocks in between. The SU is denoted as the domain $\Omega = \Omega_f \cup \Omega_m$ of which the fracture part is denoted as Ω_f and the matrix part as Ω_m.

The coordinates are denoted by $\mathbf{x_b}$ for the global scale and by $\mathbf{x_s}$ for the local scale. By letting ∂ denote *boundary of*, the matrix-fracture interface will be denoted by $\partial\Omega_m$. Let $\mathbf{n}$ denote the outward unit normal vector to this surface ($\partial\Omega_m$) pointing from the matrix to the fracture.

The second step in homogenization is to describe the transport equations on the local scale, i.e., in fractures and matrix blocks:

$$\frac{\partial}{\partial t}\left(\varphi_f^* \rho_{\alpha,f} S_{\alpha f}\right) = \nabla\cdot\left(\rho_{\alpha,f}\lambda_{\alpha f}^* \nabla\Phi_{\alpha f}\right) \text{ in } \Omega_f, \qquad \frac{\partial}{\partial t}\left(\varphi_m \rho_{\alpha,m} S_{\alpha m}\right) = \nabla\cdot\left(\rho_{\alpha,m}\lambda_{\alpha m}\nabla\Phi_{\alpha m}\right) \text{ in } \Omega_m. \tag{2}$$

These equations are found by combining the mass balance equation and Darcy's equation. At the interface $\partial\Omega_m$, there is a continuity of oil flow and water flow:

$$\left(\rho_{\alpha,f}\lambda_{\alpha f}^*\nabla\Phi_{\alpha f}\right)\cdot\mathbf{n} = -\left(\rho_{\alpha,m}\lambda_{\alpha m}\nabla\Phi_{\alpha m}\right)\cdot\mathbf{n}, \quad \text{and} \quad P_{cf}^*\left(S_{wf}\right) = P_{cm}\left(S_{wm}\right) \quad \text{on } \partial\Omega_m. \tag{3}$$

Indeed, there is a continuity of flux and capillary pressure at this interface unless one of the phases in the fracture or matrix system is immobile. Flux continuity follows from fluid conservation at the interface between fracture and matrix.

The third step is that the differentiation in the model equation is split in a global scale (big) term, ∇_b, and a local scale (small) term, where $\nabla = \nabla_b + \nabla_s$. The matrix equation acts at the local scale. Therefore, it is only necessary to apply this splitting procedure for the fracture equation. It is assumed that the contribution of differentiation at the local scale $\nabla_s(*)$ is one order of magnitude larger than the contribution of differentiation at the global scale $\nabla_b(*)$. In previous papers (Namdar Zanganeh et al. 2007; Bruining and Darwish 2006), we erroneously stated that these terms were of the same order of magnitude. However, this does not affect any of the results.

Subsequently, the transport equations are non-dimensionalized by inspection (Shook et al. 1992). In the non-dimensionalizing procedure, the first step is to write dependent and independent variables, X, as $X = X_R X_D + X_{off}$, where X_R is a reference quantity and X_{off} is an offset. The reference quantities either assume values that can be indicated in the problem of interest or made up by combining the reference quantities. In our model, we use l and L as the local and global reference (characteristic) lengths for differentiation. This results in $\nabla_D = \nabla_b + \varepsilon^{-1} \nabla_s$. The reference pressure, P_R, is the pressure difference between injection and production well (ΔP). k_R is the reference permeability, and $t_R = L^2 \mu_w / (k_R \Delta P)$ acts as the reference time for the fracture system. The new dimensionless potential (divided by p_R) is equal to the dimensionless pressure plus a rescaled gravity term: $\Phi_{\alpha f} = p_{\alpha f} + \rho_{\alpha f} g L z_D / \Delta P$ where z_D is the dimensionless vertical distance using L as the reference length. Eq. 2 has ρ_α as a common factor; therefore, it can be ignored in the non-dimensionalization procedure.

Afterwards, the reference and other quantities in each of the terms are grouped such that a dimensionless equation is obtained. This procedure leads to a dimensionless equation (with dimensionless dependent and independent variables) with some dimensionless numbers such as the permeability ratio. This ratio is defined as the intrinsic fracture permeability to the matrix permeability. We will only consider a single case for the ratio of the fracture to matrix permeability (see section 2.1). The other dimensionless number appearing in the equations is the scaling ratio ε. Different upscaled equations are obtained when dimensionless numbers assume values of different orders of magnitude with respect to ε. After non-dimensionalizing Eq. 2, it reduces to:

$$\frac{\partial}{\partial t}\left(\varphi_f^* S_{\alpha f}\right) = \nabla_b \cdot \frac{k_f^* k_{r\alpha,f}}{\mu_{\alpha,f}} \left(\nabla_b \Phi_{\alpha f} + \frac{1}{\varepsilon} \nabla_s \Phi_{\alpha f} \right) + \frac{1}{\varepsilon} \nabla_s \cdot \frac{k_f^* k_{r\alpha,f}}{\mu_{\alpha,f}} \left(\nabla_b \Phi_{\alpha f} + \frac{1}{\varepsilon} \nabla_s \Phi_{\alpha f} \right) \quad \text{in } \Omega_f . \tag{4}$$

The subscript D is dropped for reasons of concise notation.

In the same way, we derive Eq. 5 from the matrix equation (Eq. 2) by assuming that the differentiation with respect to the local scale is only relevant for the matrix equation and using the same reference time as in the fracture equation:

$$\frac{\partial}{\partial t}\left(\varphi_m S_{\alpha m}\right) = \frac{1}{\varepsilon^2} \nabla_s \cdot \left(\lambda_{\alpha m} \nabla_s \Phi_{\alpha m} \right) \quad \text{in } \Omega_m . \tag{5}$$

At the interface $\partial\Omega_m$, there is a continuity of oil and water flux. The boundary condition, Eq. 3, is rescaled similarly, i.e.,

$$k_f^* k_{r\alpha,f} \left(\nabla_b + \frac{1}{\varepsilon} \nabla_s \right) \Phi_{\alpha f} \cdot \mathbf{n} = -k_m k_{r\alpha,m} \frac{1}{\varepsilon} \nabla_s \Phi_{\alpha m} \cdot \mathbf{n} \quad \text{on } \partial\Omega_m . \tag{6}$$

In this contribution, we assume that the density and viscosity are uniform and constant.

In the fourth step, we expand the dependent variables into the contributions of decreasing significance with respect to ε:

$$\xi = \xi^{(0)} + \varepsilon \xi^{(1)} + \varepsilon^2 \xi^{(2)} + \ldots , \tag{7}$$

where ξ denotes either the saturation or the potential. Substitution of these series into the dimensionless equations results in equations consisting of terms with different orders of magnitude with respect to ε (Eq. 7 is substituted into Eqs. 4 through 6). Because the upscaling procedure should also be valid for ε values that are slightly smaller or larger than its reference value of ε, it is stated that each of the terms with a specific order of ε constitutes an equation that is separately satisfied. First, the equation of the lowest order in ε is solved leading to the solutions of the most significant contributions of the dependent variables. This means that the $1/\varepsilon^2$ terms of Eq. 4 and the $1/\varepsilon$ term of Eq. 6 with Eq. 7 lead respectively to:

$$\frac{1}{\varepsilon^2} \nabla_s \cdot k_{r\alpha,f}^{(0)} \nabla_s \Phi_{\alpha f}^{(0)} = 0 \quad \text{and} \quad \frac{1}{\varepsilon} k_{r\alpha,f}^{(0)} \nabla_s \Phi_{\alpha f}^{(0)} \cdot \mathbf{n} = 0 , \tag{8}$$

where we used the fact that $k_f^*/k_m \sim 1/\varepsilon^2$. Periodic boundary conditions in the system of Eq. 8 have a unique solution that ensures that each phase potential is constant on the local scale. Under static conditions (see, however, Hassanizadeh et al. 2002), this would mean that there is capillary-gravity equilibrium in the small unit, unless one of the phases is immobile.

Subsequently, it is possible to show that the equation with one order higher in ε (ε^{-1} terms of Eq. 4 and ε^0 terms of Eq. 6), is a linear elliptic problem for $\nabla_s\Phi_{\alpha f}^{(1)}$ in terms of $\nabla_s\Phi_{\alpha f}^{(0)}$. Constructing a relation between these two terms gives another system of differential equations that can be used to estimate $\Phi_{\alpha f}^{(1)}$ (see appendix A). The third system (ε^0 terms of Eq. 4 and ε^1 terms of Eq. 6) is the most important system because when averaged, it gives the most significant upscaled model:

$$\frac{\partial}{\partial t}\left(\varphi_f^* S_{\alpha f}^{(0)}\right) = \nabla_b \cdot \frac{k_f^* k_{r\alpha,f}^{(0)}}{\mu_{\alpha,f}}\left(\nabla_b \Phi_{\alpha f}^{(0)} + \nabla_s \Phi_{\alpha f}^{(1)}\right) + \nabla_b \cdot \frac{k_f^* k_{r\alpha,f}^{(1)}}{\mu_{\alpha,f}} \nabla_s \Phi_{\alpha f}^{(0)} + \nabla_s \cdot \frac{k_f^* k_{r\alpha,f}^{(0)}}{\mu_{\alpha,f}}\left(\nabla_b \Phi_{\alpha f}^{(1)} + \nabla_s \Phi_{\alpha f}^{(2)}\right) +$$
$$+ \nabla_s \cdot \frac{k_f^* k_{r\alpha,f}^{(1)}}{\mu_{\alpha,f}}\left(\nabla_b \Phi_{\alpha f}^{(0)} + \nabla_s \Phi_{\alpha f}^{(1)}\right) + \nabla_s \cdot \frac{k_f^* k_{r\alpha,f}^{(2)}}{\mu_{\alpha,f}} \nabla_s \Phi_{\alpha f}^{(0)} \qquad \text{in } \Omega_f. \tag{9}$$

The corresponding boundary condition with terms ε^1 reads:

$$\frac{k_f^* k_{r\alpha,f}^{(0)}}{\mu_{\alpha,f}}\left(\nabla_b \Phi_{\alpha f}^{(1)} + \nabla_s \Phi_{\alpha f}^{(2)}\right)\cdot \mathbf{n} + \frac{k_f^* k_{r\alpha,f}^{(1)}}{\mu_{\alpha,f}}\left(\nabla_b \Phi_{\alpha f}^{(0)} + \nabla_s \Phi_{\alpha f}^{(1)}\right)\cdot \mathbf{n} = -\frac{1}{\varepsilon^2}\frac{k_m k_{r\alpha,m}^{(0)}}{\mu_{\alpha,m}} \nabla_s \Phi_{\alpha m}^{(0)} \cdot \mathbf{n} \qquad \text{on } \partial\Omega_m. \tag{10}$$

It is possible to average the equations over a small unit. Here we use the notation <**q**> for the spatial average of any parameter **q**, over a small unit, i.e.

$$\langle \mathbf{q} \rangle = \frac{\mathbf{1}}{|\Omega|}\int_{\Omega_f} \mathbf{q}\, d\mathbf{x}_s. \tag{11}$$

In particular, considering the assumption of periodic local variations, the application of Gauss' theorem leads to:

$$\frac{\mathbf{1}}{|\Omega|}\int_{\Omega_f} \nabla_s \cdot \mathbf{q}\, d\mathbf{x}_s = -\frac{\mathbf{1}}{|\Omega|}\int_{\partial\Omega_m} \mathbf{q}\cdot\mathbf{n}\, d\sigma = -\frac{\mathbf{1}}{|\Omega|}\int_{\Omega_m} \nabla_s \cdot \mathbf{q}\, d\mathbf{x}_s. \tag{12}$$

In this equation, σ denotes the coordinates of the boundary, $\partial\Omega_m$. It should be noted that **n** is the outward unit normal vector to this surface ($\partial\Omega_m$) pointing from the matrix to the fracture. The contributions from the outer boundary of **Ω** cancel because **q** is considered **Ω** periodic.

We obtain the averaged zeroth order upscaled equation in three steps. First, we apply Eq. 12 to Eqs. 5, 9 and 10. Then, we consider that the terms containing $\nabla_s\Phi_{\alpha m}^{(0)}$ are zero and lastly, we substitute Eqs. 10 and 5 into Eq. 9, i.e.,

$$\frac{\partial}{\partial t}\left(\varphi_f S_{\alpha f}^{(0)}\right) + \frac{\partial}{\partial t}\frac{1}{|\Omega|}\int_{\Omega_m}\left(\varphi_m S_{\alpha m}^{(0)}\right) d\mathbf{x}_s = \nabla_b \cdot \frac{k_f k_{r\alpha,f}^{(0)}}{\mu_{\alpha,f}} \nabla_b \Phi_{\alpha f}^{(0)} \qquad \text{in } \Omega_f, \tag{13}$$

where we derived the effective fracture permeability tensor (see appendix A) and the global fracture porosity as follows

$$k_f = \frac{1}{|\Omega|}\int_{\Omega_f} k_f^*\left(\mathbf{I} + \nabla_s \otimes \omega\right) d\mathbf{x}_s, \qquad \text{and} \qquad \varphi_f = \frac{|\Omega_f|}{|\Omega|}\varphi_f^*.$$

The dyadic product $\nabla_s \otimes \omega$ is a tensor with components $\partial\omega_j / \partial x_i$ where i,j denote the x, y, z coordinates. Arbogast (1993) has derived similar equations for special cases previously. The zeroth-order upscaled equation (Eq. 13) describes the global displacement process through a globally equivalent homogeneous medium characterized by effective coefficients, i.e., φ_f and k_f.

2. Dimensionless numbers

One of the advantages of homogenization is that it generates different upscaled models when characteristic dimensionless numbers assume values of different orders of magnitude with respect to ε. In this case, where we are only dealing with the zeroth-order upscaled equation, we use the ratio between the fracture and matrix permeability as the characteristic

dimensionless number. Other dimensionless numbers follow from the upscaled model equations. For these equations we can additionally define the gravity number, i.e., gravity force over viscous force, and the Peclet number. The Peclet number is defined as the ratio between the time required to imbibe water into the matrix block and the travel-time of water in fracture system. Here, all relevant dimensionless numbers playing a role both in the upscaling procedure and in the ensuing model equations are discussed.

2.1. Permeability ratio in fractures and matrix

The simplest definition of a fractured medium is a medium that contains fractures and matrix. From the fluid-flow point of view, such a medium is not necessarily a fractured medium, in particular when the matrix blocks carry a substantial part of the flow. A fractured reservoir from the fluid-flow point of view means that the total volumetric flux u_f in fractures must be substantially larger than the total volumetric flux u_m in the matrix blocks. It can be shown that the necessary requirement for this is that $k_f^* \sim \varepsilon^{-2} k_m$. Indeed, flows in the fracture and matrix are subjected to approximately the same potential gradient. In addition, the fluid viscosities in the matrix and fracture are the same. Hence, the ratio between the velocity in the fracture and the matrix u_f^* / u_m is of the order $\sim \varepsilon^{-2}$. For a statistically homogeneous medium the Darcy velocity is $u_f \sim \varphi_f u_f^*$. Because in our case the global fracture porosity (φ_f) is of the order $\sim \varepsilon$, we obtain $u_f / u_m \sim \varepsilon^{-1}$. This can be expressed in terms of permeabilities, i.e., $k_f / k_m \sim \varepsilon^{-1}$, using Darcy's law. This means that if the matrix permeability is 10 mD and $\varepsilon \sim 0.01$, the intrinsic fracture permeability k_f^* must be of the order of 100 Darcy. The order of the magnitude of the permeability ratio has also a consequence for a number of other aspects in fractured media flow. If we assume that the capillary pressure is proportional to the square root of the permeability $\sqrt{k}$, it means that for the same saturation values the capillary pressure in the matrix blocks is 100 times as large as in the fracture.

2.2 Peclet number

The Peclet number is defined as the ratio between the time required to imbibe water into the matrix block and the travel time of water in the fracture system. The derived Peclet number is based on inspection, i.e., a dimensional analysis of the model equations used (Shook et al. 1992). For our model we assume that countercurrent imbibition in the matrix is the main recovery mechanism. Flow in the fractures is governed by multi-phase convection flows. Therefore, in this model the Peclet number expresses the ratio between transport by convection (mainly viscous forces) in the fracture and the transport by capillary diffusion in the matrix. For other cases of interest, the relevant dimensionless number can be derived from the ratios of the residence time of the fluids in the matrix blocks and fractures, respectively. For our situation, we drive the following expressions for the Peclet number:

$$\mathrm{Pe} = \frac{\ell^2 u_f}{D_{cap} L}, \quad \text{where} \quad D_{cap} = -\frac{\lambda_o \lambda_w}{\lambda_o + \lambda_w} \frac{\mathrm{d}P_c}{\mathrm{d}S_w}. \tag{14}$$

Here λ_α is the mobility of phase α (oil, water), l is the matrix block size, and L is the distance between wells. We use u_f based on some of our simulations, although we admit that the best choice of u_f or u_f^* depends on the situation. The qualitative behavior of water-drive recovery in fractured media depends on the ratio of the characteristic time over which an amount of oil flows from the matrix to the fracture and the residence time of water in the fracture system.

If the residence time in the fracture system is small, it is expected that the recovery is controlled by the rate of countercurrent imbibition from the matrix blocks. In this case, most of the fractures contain mainly water. By capillary continuity, this sets the boundary of the matrix blocks at approximately zero capillary pressure.

If the residence time in the fracture system is large, water imbibes into the matrix blocks before reaching the production well and release an equal volume of oil (in the case of incompressible flow) to the fracture. In this case, there is a long period in which mainly oil is produced at a rate equal to the injection rate, with a very little water. After this period, water breakthrough occurs and the production performance depends on the detailed geometry of the fracture system and the well configurations. Therefore, from the fluid-flow point of view, the fractured reservoir behaves like a highly heterogeneous single-porosity reservoir rather than a dual-porosity fractured reservoir. The heterogeneity distribution must be inferred from the properties of the fracture system.

2.3. Ratio of gravity to viscous forces (Gravity number)

The gravity number is defined as the ratio between the gravity forces and the viscous forces. For the zeroth-order model, the periodic boundary condition implies that viscous forces are negligible with respect to gravity forces or capillary forces on the scale of the matrix blocks. Therefore, we define the gravity number on the global (reservoir) scale. The zeroth-order model follows from the most significant terms in the transport equations, i.e., those that scale with ε^0. We assert that this model is sufficiently accurate to grasp the essential features of flow in dual-porosity reservoirs.

The typical gravity number is defined as:

$$N_G = \frac{k_f^* \Delta\rho\, gH}{\mu\, u_f^* L}, \tag{15}$$

where H is the height of the reservoir. Considering that capillary diffusion transport is known, the Peclet number is specified by the viscous forces in the fracture system. If the Peclet number is large, the viscous forces of the fracture system dominate gravity forces in the fracture system. On the other hand, when the Peclet number is small and injection is over the entire height of the reservoir, gravity forces become dominant in the fracture system. This means that for this case water tend to under-ride especially for high mobility ratios and gravity segregation happens.

3. Results and discussion

This section compares the results between the *homogenized* model, the *effective permeability* model (obtained from homogenization), and computations by ECLIPSE, which are based on the Warren and Root model. Appendix A describes the derivation of the *effective permeability* and appendix B describes the numerical *homogenized* model. The *homogenized* model (see **Fig. 2**) contains ten grid blocks in the x-direction, five grid blocks in the y-direction and three grid blocks in the z-direction. The matrix in each grid block is represented by a single representative matrix block, which is in turn discretized into $9 \times 9 \times 9$ grid blocks. The *effective permeability* model and ECLIPSE also use a discretization into $10 \times 5 \times 3$ grid blocks. In other words, we use 109500 grid blocks for the *homogenized* model. **Table 1** gives the data used to compare the *homogenized* model, the *effective permeability* model and ECLIPSE. **Fig. 3** shows the capillary pressure curve for matrix and fracture, and **Fig. 4** shows oil and water relative permeability curves for matrix and fracture.

In the simulations we vary the Peclet number (rate of water injection), while keeping the other properties constant. We base our comparison on cumulative oil and water production. The production rates can be estimated from the cumulative production curve by differentiation with respect to time. We investigate the effect of increasing the number of grid blocks for the case (Pe = 0.51, $N_G = 0.14$, $q_w = 0.1$ PV per year) because we anticipate that this result is most sensitive to grid block refinement. The result is shown in **Fig. 5**. From this we conclude that our choice of grid cell refinement is somewhat coarse for accurate results that include gravity, but sufficient for making comparisons between the models. Note that the scale in Fig. 5 differs from that in the other figures below.

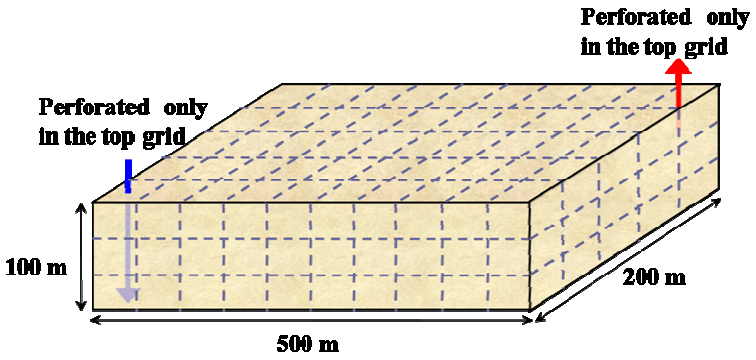

Fig. 2- Reservoir water flooding pattern and geometry in the numerical example

Table 1- Data used in the simulations

Initial reservoir pressure (MPa)	27.5	Matrix permeability, k_m, (mD)	1
Bottom hole pressure for production wells (MPa)	26.9	Oil viscosity, μ_o, (Pa.s)	0.002
Well radius (m)	0.1524	Oil density, ρ_o, (Kg/m^3)	833
Fracture aperture (μm)	100	Water viscosity, μ_w, (Pa.s)	0.0005
Local fracture porosity, φ_f^*	1	Water density, ρ_w, (Kg/m^3)	1025
Intrinsic fracture permeability, k_f^*, (D)	844	Oil residual saturation in matrix	0.3
Global fracture porosity, φ_f	1.5×10^{-4}	Oil residual saturation in fracture	0
Effective fracture permeability, k_f, (mD)	84.43	Connate water saturation in matrix	0.25
Matrix block size, l, (m)	2	Connate water saturation in fracture	0
Matrix porosity, φ_m	0.19		

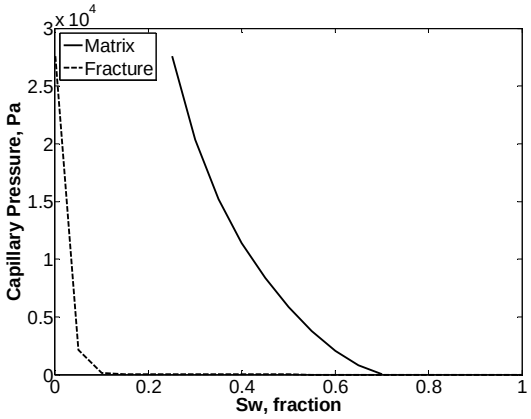

Fig. 3- Capillary pressure curve for fracture and matrix

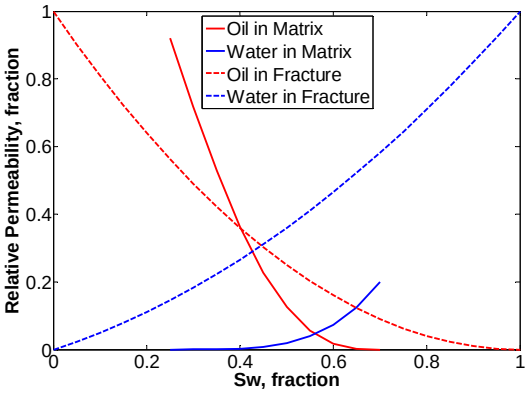

Fig. 4- Oil and water relative permeability curve for fracture and matrix

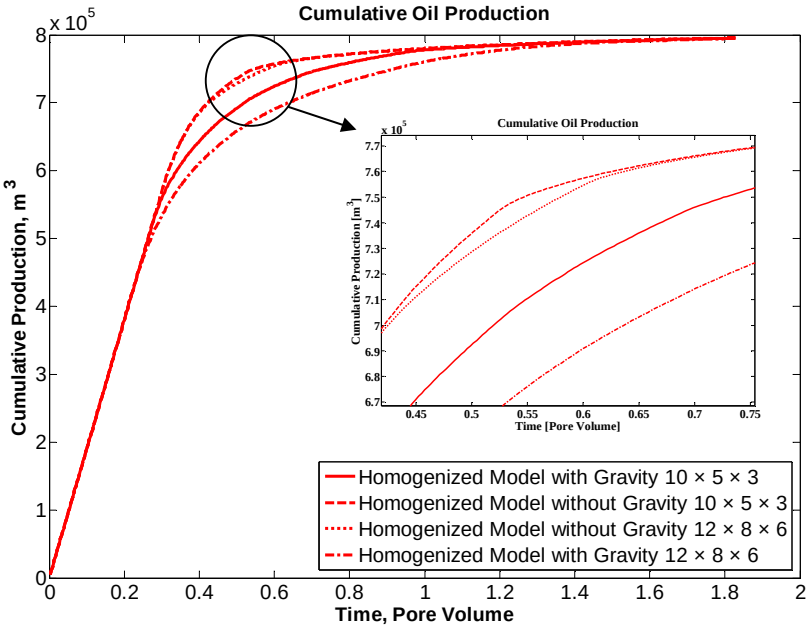

Fig. 5- Effects of refinement for the number of fracture system grid blocks on the cumulative of oil production

Figs. 6a through 6d show a comparison of the cumulative oil and water production for the *homogenized* case and the *effective permeability* case. For a low Peclet number (0.14) (**Fig. 6a**) we observe that the *homogenized* model initially predicts less, but produces more when more than 80% of one pore volume is injected. At a slightly higher Peclet number (**Fig. 6b**); we observe that the *homogenized* model and *effective permeability* model almost coincide. At higher Peclet numbers (**Figs. 6c and 6d**), the discrepancy between the *homogenized* model and the *effective permeability* model increases, where the *homogenized* model predicts a recovery that is almost two times smaller.

When the Peclet number is small, it means that the rate of oil and water exchange at the interface between matrix block and fracture is high. In this case, the residence time in the fracture system is large and water will largely imbibe in the matrix blocks and release an equal volume of oil to the fracture. Therefore there will be a long period that mainly oil is produced at a rate equal to the injection rate, with only very little water (Fig. 6a). It should be noted that for the *effective permeability* model we solved the equations, which correspond to a single conventional porosity model, with porosity equal to the matrix porosity and permeability equal to the *effective permeability* obtained from homogenization. In other words, in this case we did not consider both the fracture system and the matrix system simultaneously. Therefore, the *effective permeability* model takes a few hundred times less time than the *homogenized* model from a computational point of view.

On the other hand, when the Peclet number is large, it means that the rate of oil and water exchange at the interface between the matrix block and the fracture is low. Consequently, the residence time in the fracture system is small. Therefore, it is expected that the recovery will be controlled by the rate of countercurrent imbibition from the matrix blocks. In this case, most of the fractures contain mainly water. By capillary continuity this situation sets the boundary of the matrix blocks at the approximately zero capillary pressure, leading to a water saturation of 1 - S_{or}. As a result of this there will be short period that mainly oil is produced (**Fig. 6d**) after which oil production becomes very slow.

Note that at very low Peclet numbers (Fig. 6a) the discrepancy between the homogenized model and the effective permeability model is larger than for intermediate Peclet numbers (Fig. 6b). This is attributed to gravity segregation as discussed in section 2.3.

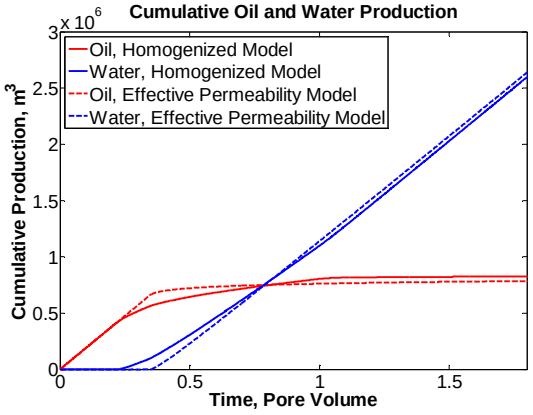

Fig. 6a- Pe= 0.14, q_w = 0.01 PV per year, K_m = 1 mD

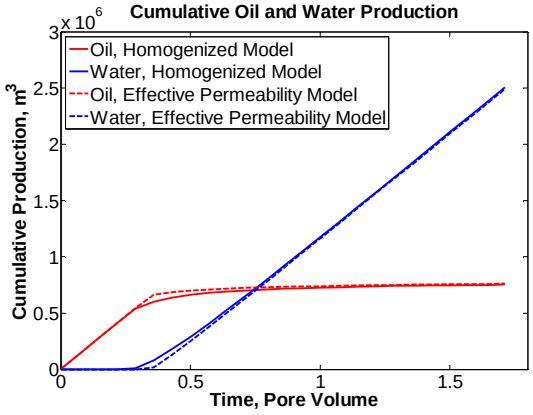

Fig. 6b- Pe= 0.79, q_w = 0.5 PV per year, K_m = 1 mD

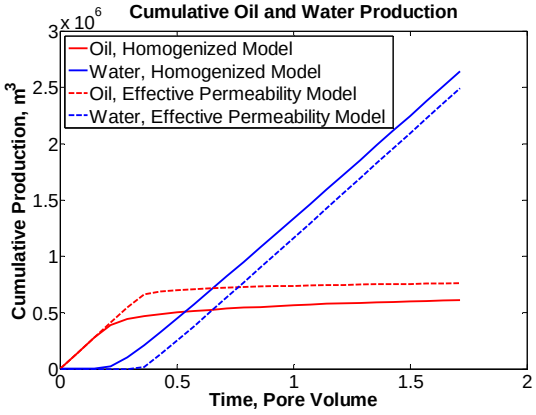

Fig. 6c- Pe= 5.61, q_w = 5.0 PV per year, K_m = 1 mD

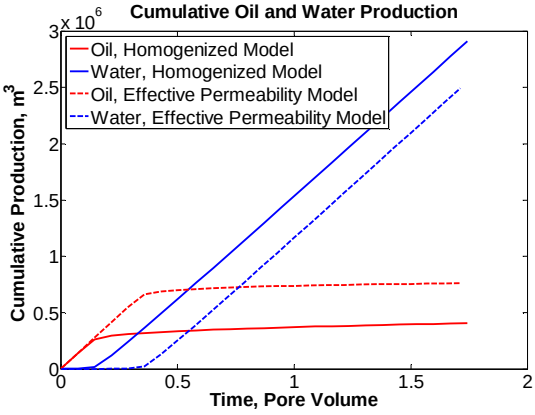

Fig. 6d- Pe= 1152, q_w = 100.0 PV per year, K_m = 1 mD

Figs. 7a through 7d show a comparison of the cumulative oil and water production for the *homogenized* model and ECLIPSE simulator. For a low Peclet number (0.14, **Fig. 7a**) we observe that at an early stage (t < 0.25 Pore Volume) the cumulative production of oil and water for both the *homogenized* model and the computation of ECLIPSE simulator are the same. At the intermediate stage (0.25 Pore Volume < t < 0.6 Pore Volume) the *homogenized* model predicts less oil production than ECLIPSE. Subsequently, at t > 0.6 pore volume the *homogenized* model predicts a higher oil production than the ECLIPSE simulator as illustrated by the fact that the slope of cumulative oil production curve for the *homogenized* model at this stage is steeper than the slope of the cumulative oil production curve for the ECLIPSE. Finally, both the *homogenized* model and ECLIPSE results tend to same value of water and oil production. The discrepancy in Fig. 7a between the *homogenized* model and ECLIPSE is due to the large gravity effects, which requires again an accurate representation of the matrix-fracture interaction.

For slightly higher Peclet number (**Fig. 7b**) we see that the cumulative of oil and water production for the *homogenized* model and ECLIPSE simulator almost coincide. Therefore, in this condition the *homogenized* model can be replaced by the Warren and Root approach without appreciable loss of accuracy.

The results at still higher Peclet numbers are shown in **Figs. 7c and 7d**. In these cases, the *homogenized* model predicts a

higher oil production at an early stage than the ECLIPSE simulator because of the depletion of oil from the part of the matrix block adjacent to the fracture resulting from of continuity of the capillary pressure. Afterwards, the predicted rate of oil production of ECLIPSE becomes more than the rate of oil production of the *homogenized* model and gradually the cumulative production of oil and water from the ECLIPSE simulator reach the value of the cumulative of oil and water production for the *homogenized* model. It should be mentioned that for Pe = 5.61 this was only observed after five pore volumes of water injection (not shown in Fig. 7d).

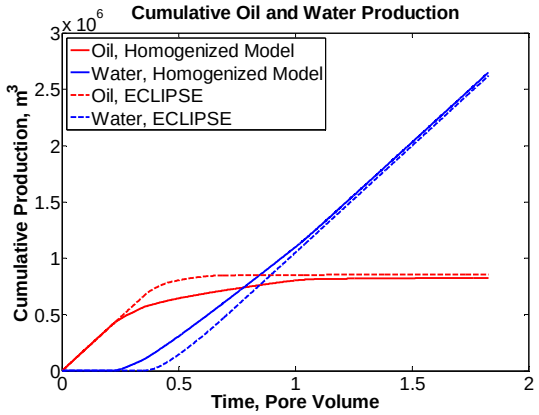

Fig. 7a- Pe= 0.14, q_w = 0.01 PV per year, K_m = 1 mD

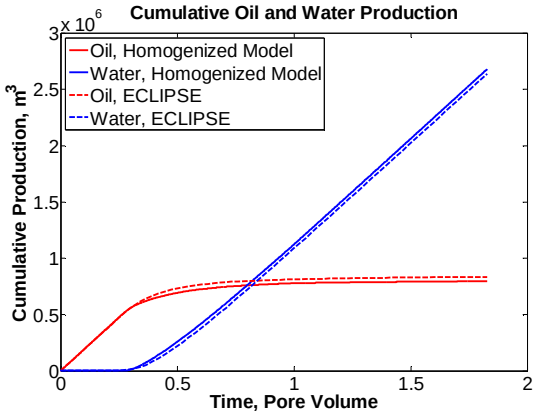

Fig. 7b- Pe= 0.51, q_w = 0.1 PV per year, K_m = 1 mD

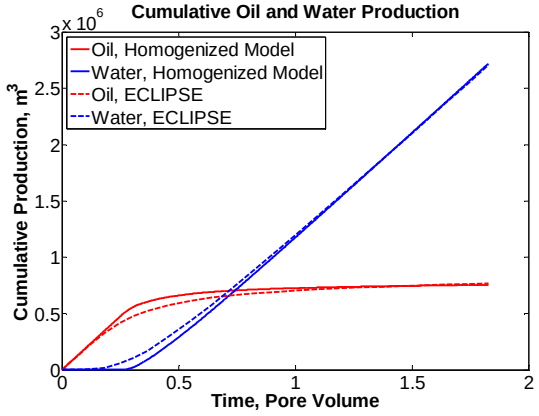

Fig. 7c- Pe= 0.79, q_w = 0.5 PV per year, K_m = 1 mD

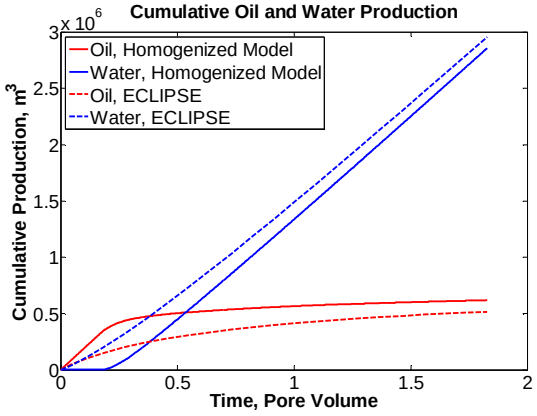

Fig. 7d- Pe= 5.61, q_w = 5.0 PV per year, K_m = 1 mD

The most important reason to see the discrepancy between the *homogenized* model and ECLIPSE model is due to the difference between the Warren and Root transfer function and the transfer function based on homogenization. The second most important reason is that the possibility of three-dimensional matrix block subgridding to the best of our knowledge is not available in the ECLIPSE simulator. We observe that most of the discrepancy between the *homogenized* model and ECLIPSE simulator happens at a higher Peclet number. In this case, accurate transfer functions are a *sine qua non* for the accurate prediction of oil recovery because the oil recovery is controlled by the rate of the countercurrent imbibition process. Consequently, satisfying the continuity of the capillary pressure has a significant effect on the cumulative production of oil and water.

Note that, as before in Fig.6a, at very low Peclet numbers (Fig. 7a) the discrepancy between the *homogenized* model and ECLIPSE is larger than for intermediate Peclet numbers (Figs. 7b and 7c).

Figs. 6a, 6b, 7b and 7c show a very small difference between the *homogenized* model and the *effective permeability* model. Hence, we can use the effective permeability model instead of using the homogenized model when the Peclet number is small (Pe < 1), but not so small that gravity starts to dominate. It should be mentioned that the *effective permeability* model can be easily implemented and can be efficiently run, i.e., with little computational time. We explain this observation using two different regimes. When the Peclet number is small, we are in a regime where the rate of fluid transport in the fracture controls the oil recovery mechanism. Therefore, in this regime, considering a precise rate of fluid exchange at the interface between matrix and fracture is not required for the prediction of oil recovery from waterflooded fractured reservoirs. For this reason, one can use either the *effective permeability* model or the Warren and Root approach. On the other hand, Figs 6c, 6d and 7d

show a large difference between the *homogenized* model and either the *effective permeability* model or the Warren and Root approach. Therefore, we must use the *homogenized* model when the Peclet number is large. A critical Peclet number marks the boundary between two regimes. If the Peclet number is large, the full-homogenized model must be used. In this regime, the oil recovery mechanism is controlled by the rate of countercurrent imbibition from the matrix blocks. In this case, the exchange rate between matrix and fracture is better described by the physically based homogenization approach than by the semi-empirical Warren and Root approach. It should be noted that the *effective permeability* model does not have an exchange term because it is a single porosity model.

A comparison of the cumulative production of oil and water for the *homogenized* model with gravity and the *homogenized* model without gravity force is shown in **Figs. 8a through 8d.** For low Peclet number it can be seen from **Fig. 8a** that at an early stage both the *homogenized* model with gravity force and the *homogenized* model without gravity force predict the same oil production, but later on water breakthrough occurs earlier for the *homogenized* model with gravity and hence leads to less oil production. When gravity forces are considered, under-riding of water occurs. At a slightly higher Peclet number (see **Fig. 8b**) we observe that the effect of gravity forces become less and for much higher Peclet numbers (**Figs. 8c and 8d**) the results of the *homogenized* model with gravity and the *homogenized* model without gravity almost coincide. The relatively small effect of gravity can be attributed to the fact that both capillary imbibition forces and viscous forces act against gravity forces. The capillary imbibition forces are constant for every case considered here. Moreover, gravity forces are also constant because the size of the reservoirs and the density difference between oil and water are kept constant. The viscous forces change on the global scale because we vary the rate of water injection for each Peclet number. When the Peclet number is small, the viscous forces are also small and therefore the effects of gravity forces can be observed. On other hand, when we go to high Peclet numbers, the viscous forces become one order of magnitude larger than gravity forces. Hence, the viscous forces become dominant and considering gravity forces for these cases does not have large impact on the cumulative production oil and water.

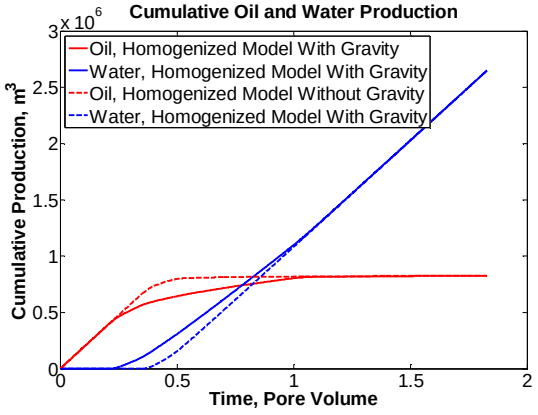

Fig. 8a- Pe = 0.14, N_G = 1.51, q_w = 0.01 PV per year

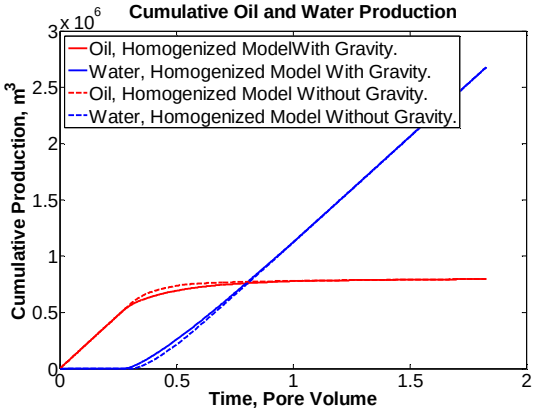

Fig. 8b- Pe = 0.51, N_G = 0.14, q_w = 0. 1 PV per year

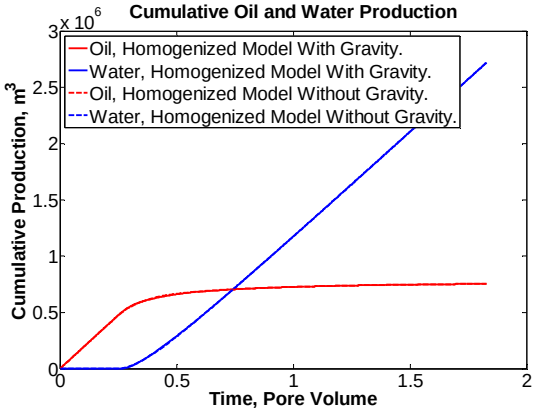

Fig. 8c- Pe = 0.79, N_G = 0.03, q_w = 0.5 PV per year

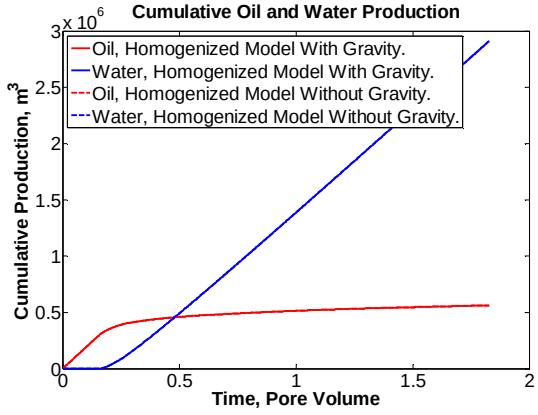

Fig. 8d- Pe = 13.54, N_G = 0.001, q_w = 10.0 PV per year

Conclusions

- Physical concepts underlie the assumptions used in homogenization.
- The method does not require intuitive closure relations, but requires order of magnitude estimates of the characteristic (dimensionless) numbers to obtain the upscaled equations.
- In general, homogenization is an upscaling method with the advantage that it finds an appropriate upscaled equation for each parameter subspace in which the characteristic dimensionless numbers assume values of a certain order of magnitude with respect to the upscaling factor.
- The most important dimensionless numbers are (a) the ratio between fracture and matrix permeability, and (b) the Peclet number, which describes the ratio between counter-current imbibition time and residence time in the fractures. A requirement for a dual-porosity model to be valid is that the intrinsic fracture permeability is two orders of magnitude larger with respect to the scaling factor than the matrix permeability.
- We derived a fully implicit 3-D numerical model for the *homogenized* equations and implemented the numerical model in a computer code.
- The results show that
    a. The discrepancy between an *effective permeability* (homogeneous) model and a dual-porosity *homogenized* model increases from negligible at low Peclet numbers to increasingly significant at higher Peclet numbers, except at very low peclet number when gravity dominates.
    b. A comparison with commercial software (ECLIPSE) shows that also only at low Peclet number there is good agreement between the simulator and our numerical results.
    c. Gravity forces at high Peclet number and low gravity number do not have a large impact on the cumulative of oil and water production.
- In view of the physical basis of homogenization, we assert that improved fracture modeling can be found based on homogenization.
- The *homogenized* model represents the physics of the problem better than the Warren and Root approach or the *effective permeability* model, which is actually a single porosity model. However, the computations with the *homogenized* model are time consuming as explained in appendix B. Therefore, it is important to discern the condition, i.e., the Peclet number, when the effective permeability model without appreciable loss of accuracy can replace the dual-porosity model. For the same conditions, it is also possible to use the Warren and Root approach.

Nomenclature

D_{cap} = Capillary-Diffusion coefficient
g = Gravity acceleration
q = Any parameter or water injection rate
k = Permeability [mD]
l = Matrix block size
L = Grid block size or reservoir length
H = Height of the reservoir
$\mathbf{n}$ = Outward unit normal vector
N_G = Gravity number
p = Pressure
p_c = Capillary pressure
$\mathbf{x_b}$ = Global coordinate
$\mathbf{x_s}$ = Local coordinate
S = Saturation
S_{or} = Residual oil saturation
t = Time
u = Velocity
$\mathbf{u}$ = Velocity vector
X = Dependent or independent variable
z = Vertical upward direction

Greek

α = Phase (Oil / Water)
ε = Scaling ratio
λ = Fluid relative mobility
μ = Viscosity
ξ = Potential / Saturation indicator
ρ = Density

σ = Coordinates of the boundary
φ = Porosity
Φ = Potential
Ω = Domain
ω =Auxiliary function

Math Signs and Operator

< > =Average sign over volume
| | =Absolute value of volume
~ =Nearly equal to
$\otimes$ =Dyadic product
$\sqrt{}$ =Square root
$\int$ =Integral
d =Differential
∂ =Partial differential
∇ =Del (gradient operator)
Δ =Delta (difference operator)
$\nabla\cdot$ = Divergence operator

Subscripts

b = Global (big) index
D = Dimensionless
f = Fracture
m = Matrix
o = Oil phase
off = Offset
r = Relative
R = Reference
s = Local (small) index
w = Water phase
α = Oil / Water index
ζ = Fracture / Matrix index

Superscripts

* = Local fracture index
(0) = Zeroth order index
(1) = First order index
(2) = Second order index

Acknowledgments

We acknowledge Maryam Namdar Zanganeh, William R. Rossen, Stefan Luthi, and Giovanni Bertotti for many useful discussions and comments. We thank Statoil for supporting this work.

References

Arbogast, T. 1993. *"Gravitational Forces in Dual-Porosity Systems. I. Model derivation by homogenization"*, Transport in Porous Media 13: 179–203.

Arbogast, T. 1993. *"Gravitational Forces in Dual-Porosity Systems. II. Computational validation of the homogenized model"*, Transport in Porous Media 13: 205–220.

Arbogast, T. 1997. *"Computational Aspects of Dual-Porosity Models"*, In U. Hornung, editor, Homogenization and Porous Media, Interdisciplinary Applied Math 203–223. New York: Springer.

Arbogast, T. and Lehr, H. L. 2006. *"Homogenization of a Darcy-Stokes System Modeling Vuggy Porous Media"*, Comput. Geosciences 10 (3): 291-302.

Barenblatt, G.E., Zheltov, I.P. and Kochina, I.N. 1960. *"Basic Concepts in the Theory of Homogeneous Liquids in Fissured Rocks"*, Journal of Applied Mathematical Mechanics 24 (5): 1286-1303.

Barenblatt, G. and Patzek, T. 2002. *"The Mathematical Model of Non-Equilibrium Effects in Water-Oil Displacement"*, SPE 75169-MS.

Bear, J. and Verruijt, A. 1987. *"Modeling Groundwater Flow and Pollution"*, Dordrecht, Netherlands: Kluwer Academic Publisher, ISBN 55608-015-8.

Bruining J. and Darwish, M.I.M. 2006. *"Homogenizeation for Fe^{2+} Deposition Near Drink Water Tube Wells during Arsenic Remediation"*, European Conference on the Mathematics of Oil Recovery X, Amsterdam, P003.

Douglas, J., Arbogast, T. and Paes Leme, P.J. 1989. *"Two Models for Waterflooding of Naturally Fractured Reservoirs"*, SPE 18425-MS.

Douglas, J. and Arbogast, T. 1990. *"Dual-Porosity Models for Flow in Naturally Fractured Reservoirs"*, In J. H. Cushman, editor, Dynamics of Fluids in Hierarchical Porous Media 177–221. Academic Press, London.

Douglas, J., Hensley, J. L. and Arbogast, T. 1991. *"A Dual-Porosity Model for Waterflooding in Naturally Fractured reservoirs"*, Comput. Methods Appl. Mech. Eng 87: 157–174.

Duijn, C.J., Molenaar, J. and Neef, M.J. 1995. *"The effect of capillary forces on immiscible two-phase flow in heterogeneous porous media"*, Transport in Porous Media 21 (1): 71-93.

Dutra, T.V. and Aziz, K. 1992. *"A New Double-Porosity Reservoir Model for Oil/Water Flow Problems"*, SPE 21248-PA.

Gasem, F.H., Nashawi, I.S., Gharbi, R. and Mir, M.I. 2008. *"Recovery performance of partially fractured reservoirs by capillary imbibition"*, Journal of Petroleum Science and Engineering 60: 39-50.

Golf-Racht, T.D. 1982. *"Fundamentals of Fractured Reservoir Engineering"*, (Vol. 12), ISBN 0-444-42046-0, Elsevier.

Hassanizadeh, M. and Gray, W. 2002. *"Dynamic Effect in the Capillary Pressure-Saturation Relationship and its Impact on Unsaturated Flow"*, Vadose Zone Journal 1: 38-57.

Kazemi, H., Seth, M.S. and Thomas, G.W. 1969. *"The Interpretation of Interference Tests in Naturally Fractured Reservoirs with Uniform Fracture Distribution"*, SPE 2156-PA.

Kazemi, H., Gilman, J.R. and Elsharkawy, A.M. 1992 *"Analytical and Numerical Solution of Oil Recovery from Fractured Reservoirs with Empirical Transfer Functions"*, SPE 19849-PA.

Lake, L.W. 1996. *"Enhanced Oil Recovery"*, ISBN-13: 978-0132816014. Prentice Hall, 1st edition.

Leverett, M.C. 1941. *"Capillary Behavior in Porous Solids"*, Trans. AIME 142: 152-169.

Namdar Zanganeh, M., Salimi, H. and Bruining, J. 2007 *"Upscaling in Fractured Reservoirs Using Homogenization"*, SPE 107383-MS

Nelson, R.A. 1985. *"A Geological Analysis of Naturally Fractured Reservoirs"*, Houson: Gulf Publishing Co.

Rossen, W.R., Gu, Y. and Lake, L.W. 2000. *"Connectivity and Permeability in Fracture networks Obeying Power statistics"*, SPE 59720-MS.

Saidi, A. M. 1975. *"Mathematical simulation model describing Iranian fractured reservoirs and its application to the Haft Kel field"*, Ninth World Petroleum Congress paper I.D. 13 (3): 209-219.

Saidi, A. M. 1983. *"Simulation of Naturally Fractured Reservoirs"*, SPE 12270-MS.

Sarma, P. and Aziz, K. 2006. *"New Transfer Functions For Simulations of Naturally Fractured Reservoirs with Dual Porosity Models"*, SPE 90231-PA.

Shook, M., LI, D. and Lake, L.W. 1992. *"Scaling Immiscible Flow Through Permeable Media by Inspectional Analysis"*, IN SITU 16 (4): 311-349.

Stearns, D.W. 1969. *"Fracture as a Mechanism of Flow in Naturally Deformed Layered Rocks"*, Conference on Research in Tectonics Proc.; Canada Geology Survey Paper, 68 (52): 79-96.

Stearns, D.W. and Friedman, M. 1972. *"Reservoirs in Fractured Rock"*, AAPG, Tulsa, OK, Memoir 16: 82-100.

Warren, J.E., and Root, P.J. 1963. *"The Behavior of Naturally Fractured Reservoirs"*, SPE 426-PA.

Yu-Shu Wu, Liu, H.H. and Bodvarsson, G.S. 2004. *"A Triple-Continuum Approach for Modeling Flow and Transport Processes in Fractured Rock"*, Journal of Contaminant Hydrology 73: 145– 179.

Appendix A. Effective fracture permeability

Collecting the terms of order $1/\varepsilon$ in Eq. 4 leads to

$$\nabla_s \cdot k_f^* k_{r\alpha,f}^{(0)} \left(\nabla_b \Phi_{\alpha f}^{(0)} + \nabla_s \Phi_{\alpha f}^{(1)} \right) = 0 \quad \text{in } \Omega_f, \tag{A-1}$$

And collecting the terms of order $\varepsilon^{(0)}$ in Eq. 6 we obtain

$$k_f^* k_{r\alpha,f}^{(0)} \left(\nabla_b \Phi_{\alpha f}^{(0)} + \nabla_s \Phi_{\alpha f}^{(1)} \right) \cdot \mathrm{n} = 0 \quad \text{on } \partial\Omega_m, \tag{A-2}$$

In order to proceed we assume that $\Phi^{(1)}{}_{\alpha f} = \boldsymbol{\omega} \cdot \mathbf{g}\mathrm{rad}_b \, \Phi^{(0)}{}_{\alpha f}$. Substitution of this in Eq. A-1 leads to

$$\nabla_s \cdot \left(k_f^* k_{r\alpha,f}^{(0)} \left(\mathbf{I} + \nabla_s \otimes \boldsymbol{\omega} \right) \cdot \nabla_b \Phi_{\alpha f}^{(0)} \right) = 0 \quad \text{in } \Omega_f, \tag{A-3}$$

where we have used that $\nabla_s \Phi^{(0)}{}_{\alpha f} = \mathbf{0}$.

And the boundary condition

$$\left(k_f^* k_{r\alpha,f}^{(0)} \left(\mathbf{I} + \nabla_s \otimes \boldsymbol{\omega}\right) \cdot \nabla_b \, \Phi_{\alpha f}^{(0)} \right) \cdot \mathbf{n} = 0 \text{ on } \partial\Omega_m, \tag{A-4}$$

In the scale of the unit cell we may assume that $\nabla_b \, \Phi^{(0)}{}_{\alpha f}$ is a vector with constant components. Therefore we may investigate the result when the unit cell is subjected to a unit potential gradient, i.e., $\nabla_b \, \Phi^{(0)}{}_{\alpha f} = \mathbf{e_x}$. In this case, Eq. A-3 reduces to

$$\nabla_s \cdot \left(k_f^* k_{r\alpha,f}^{(0)} \nabla_s \otimes \boldsymbol{\omega} \right) = 0 \quad \text{in} \quad \Omega_f, \tag{A-5}$$

And the boundary condition

$$k_f^* k_{r\alpha,f}^{(0)} \left(\nabla_s \otimes \boldsymbol{\omega}\right) = -k_f^* k_{r\alpha,f}^{(0)} \, \mathbf{I} \cdot \mathbf{n} \quad \text{on} \quad \partial\Omega_m, \tag{A-6}$$

To obtain the average fracture permeability we write the first right term of Eq. 9 after averaging

$$\begin{aligned}
\frac{1}{|\Omega|} \int_{\Omega_f} \nabla_b \cdot \frac{k_f^* k_{r\alpha,f}^{(0)}}{\mu_{\alpha j,f}} \left(\nabla_b \Phi_{\alpha f}^{(0)} + \nabla_s \Phi_{\alpha f}^{(1)} \right) d\mathbf{x}_s &= \frac{1}{|\Omega|} \int_{\Omega_f} \nabla_b \cdot \frac{k_f^* k_{r\alpha,f}^{(0)}}{\mu_{\alpha j,f}} \left(\nabla_b \Phi_{\alpha f}^{(0)} + \nabla_b \Phi_{\alpha f}^{(0)} \nabla_s \otimes \omega \right) d\mathbf{x}_s = \\
&= \frac{1}{|\Omega|} \int_{\Omega_f} \nabla_b \cdot \frac{k_f^* k_{r\alpha,f}^{(0)}}{\mu_{\alpha j,f}} \left(\mathbf{I} + \nabla_s \otimes \omega \right) \nabla_b \Phi_{\alpha f}^{(0)} d\mathbf{x}_s = \\
&= \frac{1}{|\Omega|} \int_{\Omega_f} \nabla_b \cdot \frac{k_{r\alpha,f}^{(0)}}{\mu_{\alpha j,f}} k_f^* \left(\mathbf{I} + \nabla_s \otimes \omega \right) \nabla_b \Phi_{\alpha f}^{(0)} d\mathbf{x}_s = \\
&= \nabla_b \cdot \frac{k_{r\alpha,f}^{(0)}}{\mu_{\alpha j,f}} k_f \, \nabla_b \Phi_{\alpha f}^{(0)}
\end{aligned} \tag{A-7}$$

We define the average fracture permeability as follows:

$$k_f = \frac{1}{|\Omega|} \int_{\Omega_f} k_f^* \left(\mathbf{I} + \nabla_s \otimes \omega \right) d\mathbf{x}_s. \tag{A-8}$$

Appendix B. Numerical solution

The zeroth order of upscaled two-phase flow equations based on homogenization of the fracture system is as follows

$$\begin{cases}
\varphi_f \dfrac{\partial S_{\alpha f}^{(0)}}{\partial t} + \dfrac{\varphi_m}{|\Omega|} \displaystyle\int_{\Omega_m} \frac{\partial S_{\alpha m}^{(0)}}{\partial t} dx_s - \nabla_b \cdot \left(k_f \dfrac{k_{r\alpha,f}^{(0)}}{\mu_{\alpha,f}} \nabla_b \Phi_{\alpha f}^{(0)} \right) = q_\alpha, \;\; \alpha = o, w, \\
\Phi_{\alpha f} = p_{\alpha f} + \rho_\alpha g z, \\
\Phi_{cf} = \Phi_{of} - \Phi_{wf} = p_{cf}\left(S_{wf}\right) + \left(\rho_o - \rho_w\right) g z, \\
S_{wf} + S_{of} = 1,
\end{cases} \tag{B-1}$$

where φ_f and k_f are the effective (global) fracture porosity and the effective fracture permeability respectively. The matrix equations are

$$\begin{cases}
\varphi_m \dfrac{\partial S_{\alpha m}^{(0)}}{\partial t} - \nabla_s \cdot \left(k_m \dfrac{k_{r\alpha,m}^{(0)}}{\mu_{\alpha,m}} \nabla_s \Phi_{\alpha m}^{(0)} \right) = 0, \;\; \alpha = o, w, \\
\Phi_{\alpha m} = p_{\alpha m} + \rho_\alpha g z, \\
\Phi_{cm} = \Phi_{om} - \Phi_{wm} = p_{cm}\left(S_{wm}\right) + \left(\rho_o - \rho_w\right) g z, \\
S_{wm} + S_{om} = 1, \\
\Phi_{\alpha m}\left(t, x_b, x_s\right) = \Phi_{\alpha f}\left(t, x_b\right) \qquad \text{on } \partial M.
\end{cases} \tag{B-2}$$

Although each of the systems B-1 and B-2 is posed six independent variables, two phase pressures, potentials and saturations, we can reduce this number to two. Using the volume balance relation, we can eliminate one of the saturations; moreover, the capillary pressure relation allows us to eliminate either of the two pressures. Finally, the pressures are also functions of the potentials and can be eliminated. We are thus left only to discretize the nonlinear partial differential equations.

$$\begin{cases} \varphi_f \dfrac{\partial S_{wf}}{\partial t} + \dfrac{\varphi_m}{|\Omega|}\displaystyle\int_{\Omega_m} \frac{\partial S_{wm}}{\partial t} dx_s - \nabla_b \cdot \left(k_f \dfrac{k_{rw,f}}{\mu_{w,f}} \nabla_b \Phi_{wf} \right) = q_w, \\ -\nabla_b \cdot \left(k_f \dfrac{k_{rw,f}}{\mu_{w,f}} \nabla_b \Phi_{wf} \right) - \nabla_b \cdot \left(k_f \dfrac{k_{ro,f}}{\mu_{o,f}} \nabla_b \left(\Phi_{wf} + \Phi_{cf} \right) \right) = q_w + q_o, \\ \text{No-flow boundary condition for fracture system,} \end{cases} \tag{B-3}$$

$$\begin{cases} \varphi_m \dfrac{\partial S_{wm}}{\partial t} - \nabla_s \cdot \left(k_m \dfrac{k_{rw,m}}{\mu_w} \nabla_s \Phi_{wm} \right) = 0, \\ -\nabla_s \cdot \left(k_m \dfrac{k_{rw,m}}{\mu_w} \nabla_s \Phi_{wm} \right) - \nabla_s \cdot \left(k_m \dfrac{k_{ro,m}}{\mu_o} \nabla_s \left(\Phi_{wm} + \Phi_{cm} \right) \right) = 0, \\ \left.\begin{array}{l} \Phi_{wm}\left(t, x_s, x_b\right) = \Phi_{wf}\left(t, x_b\right), \\ \Phi_{cm}\left(S_{wm}\right) = \Phi_{cf}\left(S_{wf}\right), \end{array}\right\} \quad on\ \partial M. \end{cases} \tag{B-4}$$

A backward Euler time discretization is used on the complete systems B-3 and B-4. For time level t^n, we have partial differential equations in $\mathbf{x_s}$ for each fixed $\mathbf{x_b}$ for the matrix water potential $\Phi^n{}_{wm}$ and matrix water saturation $S^n{}_{wm}$ with $\Phi^n{}_{wf}$ and $S^n{}_{wf}$ as two parameters to the system. We further discretize systems B-3 and B-4 in space by applying finite volume method. This reduces the system to a fully discrete, finite dimensional problem. Let the number of fracture unknowns be I, and denote them at time level t^n by

$$\vec{\chi}_f^n = \left\{ \Phi_{wf,i}^n, S_{wf,i}^n, i = 1, 2, ..., I \right\}.$$

The numerical method only requires a matrix block at each grid point in fracture system. Then associated to each grid point i = 1, 2, …, I, there are a series of matrix unknowns

$$\vec{\chi}_{m,i}^n = \left\{ \Phi_{wm,ij}^n, S_{wm,ij}^n, j = 1, 2, ..., J_i \right\},$$

in the ith matrix block. Let

$$\vec{\chi}_m^n = \left\{ \Phi_{wm,ij}^n, S_{wm,ij}^n, i = 1, 2, ..., I,\ j = 1, 2, ..., J_i \right\}.$$

The fully discrete nonlinear equations then take the form

$$\begin{cases} F_i\left(\vec{\Phi}_{wf}^n, \vec{S}_{wf}^n, \vec{\Phi}_{wm}^n, \vec{S}_{wm}^n\right) = 0, & i = 1, 2, ..., I, \\ M_{ij}\left(\Phi_{wf,i}^n, S_{wf,i}^n, \vec{\Phi}_{wm,i}^n, \vec{S}_{wm,i}^n\right) = 0, & i = 1, 2, ..., I,\ j = 1, 2, ..., J_i, \end{cases} \tag{B-5}$$

for some nonlinear functions F_i and M_{ij}.

One way to solve nonlinear equation of this form is to use Newton's method to linearize it. Let $\vec{\Phi}_{wf}^{n,m}, \vec{S}_{wf}^{n,m}$ *and* $\vec{\Phi}_{wm}^{n,m}, \vec{S}_{wm}^{n,m}$, denote the mth Newton iterate for the nth time level's solution, let D_π denote partial differentiation with respect to π, and let

$$F_i^{n,m-1} = F_i\left(\vec{\Phi}_{wf}^{n,m-1}, \vec{S}_{wf}^{n,m-1}, \vec{\Phi}_{wm}^{n,m-1}, \vec{S}_{wm}^{n,m-1}\right),$$
$$M_{ij}^{n,m-1} = M_{ij}\left(\Phi_{wf,i}^{n,m-1}, S_{wf,i}^{n,m-1}, \vec{\Phi}_{wm,i}^{n,m-1}, \vec{S}_{wm,i}^{n,m-1}\right),$$

and similarly for the derivatives. Then the Newton procedure can be described as the following iterative process.
1. Start with an initial guess for the solution

$$\vec{\Phi}_{wf}^{n,0}, \vec{S}_{wf}^{n,0} \text{ and } \vec{\Phi}_{wm}^{n,0}, \vec{S}_{wm}^{n,0}.$$

2. For each m = 1, 2, …, until convergence is reached:
(a) Solve for

$$\delta\vec{\phi}_{wf}^{n,m}, \delta\vec{S}_{wf}^{n,m} \text{ and } \delta\vec{\phi}_{wm}^{n,m}, \delta\vec{S}_{wm}^{n,m},$$

satisfying

$$\begin{cases} F_i^{n,m-1} + \sum_{i'}\left\{ D_{\phi_{wf,i'}} F_i^{n,m-1}\delta\phi_{wf,i'}^{n,m} + D_{S_{wf,i'}} F_i^{n,m-1}\delta S_{wf,i'}^{n,m} + \right. \\ \qquad \left. + \sum_{j'}\left[D_{\phi_{wm,i'j'}} F_i^{n,m-1}\delta\phi_{wm,i'j'}^{n,m} + D_{S_{wm,i'j'}} F_i^{n,m-1}\delta S_{wm,i'j'}^{n,m} \right]\right\} = 0, \quad i = 1,2,...,I, \\ M_{ij}^{n,m-1} + D_{\phi_{wf,i}} M_{ij}^{n,m-1}\delta\phi_{wf,i}^{n,m} + D_{S_{wf,i}} M_{ij}^{n,m-1}\delta S_{wf,i}^{n,m} + \\ \qquad + \sum_{j'}\left[D_{\phi_{wm,ij'}} M_{ij}^{n,m-1}\delta\phi_{wm,ij'}^{n,m} + D_{S_{wm,ij'}} M_{ij}^{n,m-1}\delta S_{wm,ij'}^{n,m} \right] = 0, \quad i = 1,2,...,I, \quad j = 1,2,...,J_i; \end{cases} \tag{B-6}$$

(b) Define

$$\vec{\phi}_{wf}^{n,m} = \vec{\phi}_{wf}^{n,m-1} + \delta\vec{\phi}_{wf}^{n,m}, \quad \vec{S}_{wf}^{n,m} = \vec{S}_{wf}^{n,m-1} + \delta\vec{S}_{wf}^{n,m}, \quad \vec{\phi}_{wm}^{n,m} = \vec{\phi}_{wm}^{n,m-1} + \delta\vec{\phi}_{wm}^{n,m}, \quad \vec{S}_{wm}^{n,m} = \vec{S}_{wm}^{n,m-1} + \delta\vec{S}_{wm}^{n,m}.$$

Within the linearized Newton problem, The matrix solution in the ith block is an affine operator of $\Phi^{n,m}{}_{wf,i}$ and $S^{n,m}{}_{wf,i}$. therefore, one can decouple the matrix and fracture problems. The matrix problem in Eq. B-6 is replaced by the following three problems for

$$\left(\tilde{\delta}\vec{\phi}_{wm}^{n,m}, \tilde{\delta}\vec{S}_{wm}^{n,m}\right), \quad \left(\hat{\delta}\vec{\phi}_{wm}^{n,m}, \hat{\delta}\vec{S}_{wm}^{n,m}\right), \quad \text{and} \quad \left(\bar{\delta}\vec{\phi}_{wm}^{n,m}, \bar{\delta}\vec{S}_{wm}^{n,m}\right).$$

For each i = 1, 2, …, I and j = 1, 2, …, J_i,

$$\begin{cases} D_{\phi_{wf,i}} M_{ij}^{n,m-1} + \sum_{j'}\left[D_{\phi_{wm,ij'}} M_{ij}^{n,m-1}\tilde{\delta}\phi_{wm,ij'}^{n,m} + D_{S_{wm,ij'}} M_{ij}^{n,m-1}\tilde{\delta}S_{wm,ij'}^{n,m} \right] = 0, \\ D_{S_{wf,i}} M_{ij}^{n,m-1} + \sum_{j'}\left[D_{\phi_{wm,ij'}} M_{ij}^{n,m-1}\hat{\delta}\phi_{wm,ij'}^{n,m} + D_{S_{wm,ij'}} M_{ij}^{n,m-1}\hat{\delta}S_{wm,ij'}^{n,m} \right] = 0, \\ M_{ij}^{n,m-1} + \sum_{j'}\left[D_{\phi_{wm,ij'}} M_{ij}^{n,m-1}\bar{\delta}\phi_{wm,ij'}^{n,m} + D_{S_{wm,ij'}} M_{ij}^{n,m-1}\bar{\delta}S_{wm,ij'}^{n,m} \right] = 0. \end{cases} \tag{B-7}$$

The result is that

$$\begin{aligned} \delta\phi_{wm,ij}^{n,m} &= \tilde{\delta}\phi_{wm,ij}^{n,m}\delta\phi_{wf,i}^{n,m} + \hat{\delta}\phi_{wm,ij}^{n,m}\delta S_{wf,i}^{n,m} + \bar{\delta}\phi_{wm,ij}^{n,m}, \\ \delta S_{wm,ij}^{n,m} &= \tilde{\delta}S_{wm,ij}^{n,m}\delta\phi_{wf,i}^{n,m} + \hat{\delta}S_{wm,ij}^{n,m}\delta S_{wf,i}^{n,m} + \bar{\delta}S_{wm,ij}^{n,m}. \end{aligned} \tag{B-8}$$

We thus modify step 2(a) of the Newton algorithm by first solving system of Eq. B-7. The fracture δ-potential and fracture δ-saturation are then given by solving the fracture equations of B-6, using implicitly the definition of Eq. B-8. Finally, we explicitly use the fracture δ-potential and δ-saturation and Eq. B-8 to update the matrix δ-potential and δ-saturation.